Published in final edited form as:
Biochemistry. 2012 March 13; 51(10): 2136–2145. doi:10.1021/bi300141h.

SOLUTION STRUCTURE OF THE FIRST SAM DOMAIN OF ODIN AND BINDING STUDIES WITH THE EPHA2 RECEPTOR

Flavia Anna Mercurio[‡], **Daniela Marasco**[‡,&,$], **Luciano Pirone**[$], **Emilia Maria Pedone**[&,$], **Maurizio Pellecchia**[#], and **Marilisa Leone**[&,$,*]

[‡]Department of Biological Sciences, University of Naples "Federico II", Naples, Italy

[&]Centro Interuniversitario di Ricerca sui Peptidi Bioattivi (CIRPEB), Naples, Italy

[$]Institute of Biostructures and Bioimaging, National Research Council, Naples, Italy

[#]Sanford - Burnham Medical Research Institute, La Jolla (CA) USA

Abstract

The EphA2 receptor plays key roles in many physiological and pathological events including cancer. The process of receptor endocytosis and the consequent degradation have lately attracted attention as possible means of overcoming the negative outcomes of EphA2 in cancer cells and decreasing tumor malignancy. A recent study indicates that Sam (Sterile Alpha Motif) domains of Odin, a member of the ANKS (Ankyrin repeat and sterile alpha motif domain-containing) family of proteins, are important to regulate EphA2 endocytosis. Odin contains two tandem Sam domains (Odin-Sam1 and Sam2).

Herein we report on the NMR solution structure of Odin-Sam1; through a variety of assays (employing NMR, SPR and ITC techniques), we clearly demonstrate that Odin-Sam1 binds to the Sam domain of EphA2 in the low micromolar range. NMR chemical shift perturbation experiments and molecular modeling studies point out that the two Sam domains interact with a head to tail topology characteristic of several Sam-Sam complexes. This binding mode is similar to that we have previously proposed for the association between the Sam domains of the lipid phosphatase Ship2 and EphA2.

This work further validates structural elements relevant for the heterotypic Sam-Sam interactions of EphA2 and provides novel insights for the design of potential therapeutic compounds that can modulate receptor endocytosis.

Eph receptors represent a large subgroup of receptor tyrosine kinase family and together with their ephrin ligands play relevant roles in several physiological and pathological processes (1–2). Interestingly, these receptors are differentially expressed in unhealthy *versus* normal tissues and thus, considered attractive targets in drug discovery (3). Among them, EphA2 has received a great amount of attention. The most recent work has associated EphA2 to cataracts (4–6) and entry of the hepatitis C virus into the host cell (7). However, EphA2 has long been related to cancer, and even if its role in this disease has been described

[*]To whom correspondence should be addressed: Dr. Marilisa Leone. Institute of Biostructures and Bioimaging, National Research Council, Via Mezzocannone 16, 80134, Naples, Italy. Phone: +39(081) 2534512. Fax: +39(081) 2536642. marilisa.leone@cnr.it.

[†]Odin-Sam1 NMR structures have been deposited in the Protein Data Bank under accession code 2LMR. Assigned chemical shifts of Odin-Sam1 have been deposited in the bmrb data bank under accession code 18134.

SUPPORTING INFORMATION AVAILABLE

Details about chemical shift perturbation and SPR studies with EphA2-Sam mutants; figures showing several Haddock solutions and lists of intermolecular interactions; sequence alignments of different Sam domains; figures related to the NMR displacement experiment with Ship2-Sam. This material is available free of charge via the Internet at http://pubs.acs.org

as both complex and controversial, many of its pro-cancer activities have been well characterized (1). The processes of enhanced EphA2 endocytosis and subsequent degradation have been correlated with weakened malignant cell behavior (1). Recent studies have focused on the regulation mechanisms at the basis of EphA2 receptor endocytosis (8–9). First, lipid phosphatase Ship2 (Src homology 2 domain-containing phosphoinositide-5-phosphatase 2) has been identified as a prominent regulator of this process (8). *In vitro* experiments have demonstrated that Ship2 over-expression in malignant breast cancer cells increases EphA2 stability, while decreased levels of Ship2 facilitate receptor internalization and degradation. To exert its function, Ship2 needs to be engaged at the receptor site by means of a heterotypic interaction between its sterile alpha motif (Sam) domain and the Sam domain of EphA2 (EphA2-Sam) (8).

Sam domains are protein binding modules containing~70 amino acids that form a five helix bundle and are involved in many biological processes mainly via homo and hetero-dimerization or polymerization processes(10–11).

The NMR solution structure of the Sam domain of Ship2 (Ship2-Sam, pdb id 2K4P) and binding studies with the Sam domain from the EphA2 receptor (EphA2-Sam) have previously been reported (12). ITC (Isothermal titration calorimetry) experiments have indicated that the two domains interact with a dissociation constant in the low micromolar range. Furthermore, chemical shift perturbation experiments have revealed the reciprocal binding interfaces of Ship2-Sam and EphA2-Sam and, together with modeling studies, have shown that this interaction may adopt a ML (Mid-Loop)/EH (End-Helix) model, characteristic of other Sam/Sam complexes (12–15).

A recent work indicates that EphA2 endocytosis is also regulated by ANKS (Ankyrin repeat and Sam domain containing) family proteins (9). This class of proteins includes Odin (16) and AIDA1b (AβPP intracellular domain-associated protein 1B) (17), which possess in addition to six ankyrin repeats and a PTB (phosphotyrosine binding) domain, two Sam domains in tandem (Sam1 and Sam2).

Over-expression of Odin in MDA-MB-231 human breast carcinoma cells and MEFs (Mouse embryonic fibroblast) protects EphA2 from undertaking internalization and degradation after ligand stimulation while a Sam domain deletion mutant of Odin lacks this function (9).

Herein, we describe solution structure studies of the first Sam domain of Odin (Odin-Sam1) and binding studies with EphA2-Sam. Through a variety of assays relying on NMR, SPR and ITC techniques we clearly demonstrate that Odin-Sam1 and EphA2-Sam interact with low micromolar affinity and 1:1 stoichiometry. NMR chemical shift perturbation experiments allow identification of the reciprocal binding interfaces of the two proteins; moreover, NMR-based displacement experiments and molecular docking studies show that Ship2-Sam and Odin-Sam1 share a common binding site on the surface of EphA2-Sam and adopt similar binding modes for these heterotypic Sam-Sam interactions. Our work sheds additional light on the structural features that are relevant for heterotypic Sam-Sam complexes involving EphA2 and provides novel information for the design of therapeutic compounds able to modulate receptor endocytosis.

MATERIALS AND METHODS

Protein expression

Recombinant proteins were expressed in *E. coli*. The following PET15B-constructs were used for this study: Ship2-Sam (residues 1199–1258 of human Ship2 UniprotKB/TrEMBL code: O15357), Odin-Sam1 (residues 691–770 of human Odin, UniprotKB/TrEMBL code:

Q92625), Odin-Sam2 (residues 761–840 of human Odin, UniprotKB/TrEMBL code: Q92625). Constructs designed for wild-type human EphA2-Sam (Swiss-Prot/TrEMBL: P29317), its double (H45N, R71A) and triple (K38A, R78A, Y81S) mutants have been previously described (12, 18).

Synthetic genes coding these proteins were all purchased from Celtek Bioscience (Nashville, TN) and contain an N-terminal His-tag and a thrombin cleavage site.

Genes were transformed using BL21-Gold (DE3) competent cells (Stratagene). Protein expressions and purification protocols implemented for labeled and unlabeled Sam domains production, have already been reported (18).

To express unlabeled proteins, bacteria were grown in LB medium. M9 minimal media supported with 2 g/L of ^{13}C-Glucose and/or 0.5 g/L of $^{15}NH_4Cl$ were prepared for expression of $^{15}N/^{13}C$ double labeled and ^{15}N labeled proteins respectively. M9 medium containing 3.6 g/L of ^{12}C-glucose (natural abundance) and 0.4 g/L of ^{13}C-glucose was implemented to achieve 10% fractional ^{13}C labeling for stereo-specific assignments of Leu-$CH_3^{\delta 1,2}$/Val-$CH_3^{\gamma 1,2}$ methyl groups (19). Expression protocols for uniformly or selectively labeled proteins were identical to those followed for unlabeled proteins production. Briefly, bacteria were grown at 37 °C; protein over-expression was induced at a cell optical density OD_{600}=0.6 nm by isopropyl β-D-thiogalactopyranoside (IPTG) (1 mM) at 25 °C overnight.

Proteins were purified with an AKTA Purifier FPLC system by affinity chromatography on a nickel column (GE Healthcare, Milano, Italy).

Resonance assignments

Resonance assignment experiments were acquired at 25 °C on a Varian Unity Inova 600 MHz spectrometer equipped with a cold probe. NMR samples consisted of ^{15}N or $^{15}N/^{13}C$ labeled Odin-Sam1 (~900 μM) in phosphate buffer saline (PBS, 10 mM phosphates, 140 mM NaCl, 2.7 mM KCl) (Fisher) at pH=7.7, 0.2 % NaN_3 with volumes of 600 μL (95% H_2O/5% D_2O). Backbone assignments were carried out through analysis of triple resonance experiments (HNCA, HN(CO)CACB, HNCACB) (20). Carbon side chains were identified in (H)CC(CO)NH and HCCH-TOCSY spectra. Proton side chains were assigned in the HCCH-TOCSY spectrum or by comparing 3D ^{15}N resolved-[^{1}H, ^{1}H] NOESY (100 ms mixing time) and 3D ^{15}N resolved-[^{1}H, ^{1}H] TOCSY (70 ms mixing time). Aromatic side chains were identified by combined analysis of 2D [^{1}H, ^{1}H] NOESY (mixing time 100 ms) and 2D TOCSY (mixing time 70 ms) experiments recorded with samples of Odin-Sam1 dissolved in 99% D_2O. Stereo-specific assignments for Leu-$CH_3^{\delta 1,2}$ and Val-$CH_3^{\gamma 1,2}$ groups of Odin-Sam1 were obtained from a [^{1}H, ^{13}C] HSQC experiment of a fractionally ^{13}C labeled Odin-Sam1 sample (500 μM) (19).

To obtain the nearly complete backbone resonance assignments of the Odin-Sam1/EphA2-Sam complex, HNCA and 3D ^{15}N resolved-[^{1}H, ^{1}H] NOESY (100 ms mixing time) spectra were acquired with samples containing either $^{15}N/^{13}C$ double labeled Odin-Sam1 (450 μM) and unlabeled EphA2-Sam (~1 mM), or double labeled EphA2-Sam (350 μM) and unlabeled Odin-Sam1 (900 μM).

NMR spectra were processed with Varian software (Vnmrj version 1.1D) and analyzed with NEASY (21) (http://www.nmr.ch/).

Relaxation measurements

Backbone ^{15}N longitudinal (R1) and transverse (R2) relaxation rates, were evaluated at 25 °C and 600 MHz. Measurements were taken with two ^{15}N-labeled Odin-Sam1 samples at

concentrations of 100 μM and 900 μM respectively and a sample of the Sam-Sam complex consisting of labeled Odin-Sam1 (450 μM) and unlabeled EphA2-Sam (~1 mM).

R1 and R2 relaxation data were collected as 1D spectra (4 k data points and 2 or 4 k transients). R1 data sets were recorded with the following values of the relaxation delay: 0.01, 0.1, 0.3, 0.6, 1.0 s; R2 data sets were acquired with relaxation delays: 0.01, 0.03, 0.05, 0.07, 0.09, 0.11, 0.15, 0.19 s. Average R1 and R2 values were estimated by the decrease of signal intensity as function of relaxation delays. To calculate the rotational correlation time, average R2/R1 ratios were used as input for the software tmest (A. G. Palmer III, Columbia University) (22).

DOSY (Diffusion Ordered Spectroscopy)

The diffusion-ordered NMR spectroscopy was conducted with the Pulsed Gradient Spin-Echo (PGSE) NMR technique (23). The translational self-diffusion coefficient D can be calculated with the equation: $I=I_0\exp(-D\gamma^2\delta^2G^2(\Delta-\delta/3))$ where I_0 is the measured signal intensity of a set of resonances at the smaller gradient strength and I is the corresponding observed peaks intensity, D is the diffusion constant, γ is the proton gyromagnetic ratio, δ is the diffusion gradient length, G is the gradient strength and Δ is the diffusion delay (24).

Series of spectra were acquired with 512 scans and 16 K data points. We conducted DOSY experiments with Odin-Sam1 samples at concentrations of 100 μM and 900 μM. The hydrodynamic radius *r*H of the protein was evaluated with the Stokes-Einstein equation $D_t=\frac{k_BT}{f}$, where $f= 6\pi\eta r_H$ is the translational friction coefficient, η is the viscosity of the solution, k_B is the Boltzmann constant, *T* is the temperature in K.

Structure calculations and analysis of Odin-Sam1

Analysis of a 3D ^{15}N resolved-[^{1}H, ^{1}H] NOESY-HSQC spectrum (25) (100 ms mixing time), a 3D ^{13}C resolved-[^{1}H, ^{1}H] NOESY-HSQC spectrum (100 ms mixing time) and a 2D [^{1}H, ^{1}H] NOESY (26) (100 ms mixing time), for the aliphatic to aromatic region, that was acquired after dissolving the lyophilized protein sample in 99% D_2O, was used to collect distance constraints for structure calculations. CYANA version 2.1 (27) was employed to calculate the solution structure of Odin-Sam1. Angular constraints were generated with the GRIDSEARCH module of CYANA. The final structure calculation includes 1206 upper distance constraints (393 intra-residue, 239 short-range, 275 medium-range, 299 long-range), 372 angle constraints and information on stereospecific assignments for methyl groups of Val32, Val56, Val63, Leu36, Leu48 and Leu84. Structure calculations were initiated from 100 random conformers; the 20 structures that better satisfy experimental constraints (i.e: lowest CYANA target functions) were further inspected with the programs MOLMOL (28) and iCING (http://proteins.dyndns.org/cing/iCing.html). Surface representations were generated with PVM 1.5.6rc1 (29).

NMR Binding studies

Protein-protein interaction studies were conducted by means of NMR titration experiments and analysis of 2D [^{1}H, ^{15}N] HSQC spectra. To identify Odin-Sam1 binding interface for EphA2-Sam, 2D [^{1}H, ^{15}N] HSQC spectra of ^{15}N labeled Odin-Sam1 (160 μM) were recorded for the protein in the unbound-form and after addition of unlabeled EphA2-Sam (80 μM, 160 μM, 240 μM, 400 μM). To recognize the binding site of EphA2-Sam for Odin-Sam1, 2D [^{1}H, ^{15}N] HSQC spectra of a ^{15}N labeled EphA2-Sam sample (63 μM) were recorded in the absence and presence of unlabeled Odin-Sam1 (360 μM and 600 μM).

To verify the binding of EphA2-Sam mutants to Odin-Sam1, NMR chemical shift perturbation experiments were performed with ^{15}N labeled Odin-Sam1 samples (50–100 μM concentration) and unlabeled double (H45N, R71A) and triple (K38A, R78A, Y81S) EphA2-Sam mutants (concentrations ranging from 200 μM to 2 mM) (See Supplemental Data).

Analysis of titration experiments and overlays of 2D spectra were performed with the program Sparky (T. D. Goddard and D. G. Kneller, SPARKY 3, University of California, San Francisco).

Surface Plasmon Resonance

EphA2-Sam proteins were immobilized in 10 mM acetate buffer pH=5.0 (flow rate 5 μL/min, injection time 7 min) on a CM5 Biacore sensor chip, using EDC/NHS chemistry, following the manufacturer's instructions (30). Residual reactive groups were deactivated with 1 M ethanolamine hydrochloride, pH=8.5; the reference channel was prepared by activation with EDC/NHS and deactivation with ethanolamine. Immobilization levels were: 940, 1313, 1480 RU, for wild-type EphA2-Sam, double (H45N, R71A) and triple (K38A, R78A, Y81S) mutants, respectively. Experiments were conducted at 25 °C and a constant 20 μL/min flow rate using as running buffer a solution of Hepes 10 mM, pH=7.4, NaCl 150 mM, surfactant P20 0.05% v/v (90 μL injected for each experiment). Binding experiments were carried out with Odin-Sam1 at various concentrations in the range of 0.1–400 μM. The BIA evaluation analysis package (version 4.1, GE Healthcare, Milano, Italy) was used to subtract the signal of the reference channel and to estimate K_D values. RUmax values as function of proteins concentrations were fit by non-linear regression analysis with GraphPad Prism, version 4.00 (GraphPad Software, San Diego, California) (31).

Isothermal titration Calorimetry (ITC)

ITC studies were performed at 25 °C with an iTC200 calorimeter (MicroCal/GE Healthcare, Milano, Italy). A solution of EphA2-Sam at a concentration of 257 μM was titrated into a solution of Odin-Sam1 (10 μM). Both proteins were extensively dialyzed in the same buffer (PBS, pH=7.7) prior to ITC measurements. Fitting of data to a single binding site model was conducted with the Origin software as supplied by GE HealthCare. ITC runs were repeated twice to evaluate the reproducibility of results.

Docking studies

Models of the Odin-Sam1/EphA2-Sam complex were generated with the Haddock web server (32). NMR structures (first conformers) of both Odin-Sam1 (pdb id: 2LMR) and EphA2-Sam (pdb id: 2E8N, RIKEN Structural Genomic Initiative) were used in these studies. Ambiguous interaction restraints were generated from chemical shift perturbation data. For Odin-Sam1 active residues (i.e: L49, L50, N51, F53, D54, D55, V56, H57, F58, Q67, D68, R70, D71) were chosen among those with the highest chemical shift variations because they either possess high solvent exposure or could potentially supply important intermolecular contacts as revealed by structural homologies with other Sam-Sam complexes. For EphA2-Sam, we adopted similar selection criteria for active residues (i.e: K38, R71, G74, H75, K77, R78, Y81). The C-terminal and N-terminal tails of Odin-Sam1 (residues 21–24 and 95–101 respectively) were considered fully flexible during all the docking stages, whereas the region encompassing residues 51–65 was set as semi-flexible. For EphA2-Sam fully flexible segments include the N-terminal and C-terminal tails; the portion of C-terminal α5 helix covering residues 74–84 of EphA2-Sam (corresponding to amino acids 59–69 according to the sequence numbers of the pdb id 2E8N) was considered semi-flexible.

In all of the docking runs, passive residues were set automatically by the Haddock web server and the solvated docking mode was turned on (33).

In the first iteration of the docking protocol (i.e: the rigid body energy minimization) 1000 structures were calculated, in the second iteration the 200 best solutions were subjected to semi-flexible simulated annealing, a final refinement in water was also performed.

The final 200 Haddock models were all visually inspected and solutions not compatible with our experimental data and/or containing highly unusual protein orientations were soon removed. This first selection screening reduced the number of structures to 78. The resultant solutions were further analyzed with MOLMOL (28) and compared with experimental structures of other heterotypic Sam-Sam complexes (for example the AIDA1 Sam tandem, pdb id 2KIV (34)), to recognize characteristic features. At the end of this analysis 22 models were chosen as being representative of the possible EphA2-Sam/Odin-Sam1 conformations. Solutions were clustered using a pairwise RMSD cutoff value of 2 Å and at least one structure *per* cluster. The RMSD values were calculated with MOLMOL (28) by superimposing the structures on the backbone atoms of residues 36–41, 62–65, 70–81 of EphA2-Sam and residues 48–73 of Odin-Sam1. This clusterization procedure indicated the presence of 5 families of structures in the selected ensemble (See Supplemental Data, Figure S3).

RESULTS

NMR Solution structure of Odin-Sam1

To assess the quaternary structure of Odin-Sam1 in solution, we have conducted ^{15}N R1 and R2 nuclear spin relaxation rates measurements along with DOSY (Diffusion ordered spectroscopy) experiments.

The rotational correlation time, τc, of the protein at 100 μM concentration, estimated by relaxation data (R2/R1 average value), is 7.4 ± 0.7 ns, and does not change when the protein concentration is increased to 900 μM (i.e: 7.3 ± 0.6 ns). The τc of Odin-Sam1 bound to EphA2-Sam increases instead to 11± 1 ns. DOSY measurements (23) indicate for a more diluted Odin-Sam1 sample (100 μM) a diffusion coefficient Dt equal to $(1.5 \pm 0.1)\cdot 10^{-10}$ m^2 s^{-1} and a corresponding hydrodynamic radius r_H value of 16.7 Å. For a Odin-Sam1 sample at a higher concentration (900 μM), we obtained similar diffusion parameters ($Dt=(1.40 \pm 0.07)\cdot 10^{-10}$ m^2 s^{-1} and r_H=17.5 Å).

These studies clearly demonstrate that under the experimental conditions used to calculate Odin-Sam1 NMR structure (~ 900 μM concentration) aggregation processes can be ignored.

Odin-Sam1 solution structure is a canonical Sam domain helix bundle (Figure 1), the region encompassing the α3 helix lacks ordered secondary structure elements, however, a reduced number of constraints could be collected for residues in this portion of the protein.

Relevant structural parameters for Odin-Sam1 conformers are listed in Table 1.

Odin-Sam1/EphA2-Sam interaction

Binding of Odin-Sam1 to EphA2-Sam was first monitored by means of chemical shift perturbation studies (35). 2D [^1H, ^{15}N] HSQC experiments were recorded for a ^{15}N uniformly labeled Odin-Sam1 sample in presence and absence of unlabeled EphA2-Sam (Figure 2A). Proton and nitrogen normalized chemical shifts variations were evaluated with the equation $\Delta\delta = [(\Delta H_N)^2 + (0.17 * \Delta^{15}N)^2]^{1/2}$ (Figure 2B) (36). Upon heterotypic association, many changes affect the spectrum, however the greatest Δδ (values > 0.2 ppm)

occur in the middle region of the protein, including helices α3, α4 and to a lesser extent α2 (Figures 2C, D).

Similar NMR experiments with ^{15}N labeled EphA2-Sam and unlabeled Odin-Sam1 were conducted to map the binding surface of EphA2-Sam for Odin-Sam1 (Figure 3A). We estimated normalized chemical shift deviations to identify the residues of the receptor participating in the interaction with Odin-Sam1 (Figure 3B). The largest deviations are localized at the interface between the α5 helix and the adjacent α1α2 and α4α5 loop regions (Figure 3C).

Chemical shift mapping data suggest that Odin-Sam1 and EphA2-Sam may adopt a Mid-Loop/End-Helix binding model that is characteristic of Sam-Sam complexes (13–14, 34, 37).

SPR and ITC experiments were also performed and both confirmed a clear association of Odin-Sam1 and EphA2-Sam (Figure 4). For SPR experiments, EphA2-Sam was efficiently immobilized on the chip surface while Odin-Sam1 was used as an analyte; kinetic experiments along with a plot of RUmax values of each experiment *versus* Odin-Sam1 concentration, both employing a 1:1 interaction model, provided a low micromolar dissociation constant value for the Odin-Sam1/EphA2-Sam complex (Figure 4A, B). Specifically, a K_D value of 5.5 ± 0.9 μM could be obtained by best fitting of experimental data via a non-linear regression analysis (Fig. 4B).

ITC experiments also indicated that Odin-Sam1 associated with EphA2 with 1:1 stoichiometry and a K_D=0.62 ± 0.04 μM (Figure 4C).

NMR and SPR studies with EphA2-Sam mutants (12) were conducted to gain additional insights into the mode of binding of Odin-Sam1 to EphA2-Sam (Supplemental Figures S1 and S2). Details about the design of the two mutant proteins were previously described (12). Briefly, in the triple (K38A, R78A, Y81S) EphA2-Sam mutant we mutated residues located in the α5 helix and α1α2 loop that constitute part of the putative interaction surface of EphA2-Sam for Odin-Sam1 (i.e: regions undergoing major chemical shift changes upon binding of Odin-Sam1 to the receptor) (Figures 3C and Supplemental Figure S1) and amino acids replacements were planned to destroy potential key interactions at the dimer interface without perturbing the overall protein structure. In the (H45N, R71A) EphA2-Sam construct, mutations were instead inserted in regions adjacent to the putative binding site (Figure 3C and Supplemental Figure S2).

NMR and SPR experiments revealed for the triple (K38A, R78A, Y81S) mutant a binding affinity lower than that of the wild-type protein for Odin-Sam1 (Supplemental Figure S1). On the other hand, EphA2-Sam double (H45N, R71A) mutant preserved an ability to associate with Odin-Sam1 similar to that of the wild-type protein (Supplemental Figure S2).

Molecular Modeling of the complex Odin-Sam1/EphA2-Sam

A speculative model of the Odin-Sam1/EphA2-Sam complex was built by molecular docking with the software Haddock 2.0 (32, 38) (See Materials and Methods section for details).

A representative structure (corresponding to the second best Haddock solution) is shown in Figure 5A. These modeling studies, in agreement with chemical shift perturbation data, indicated for the complex a head to tail topology also known as Mid-Loop(ML)/End-Helix(EH) binding mode (13–14), in which Odin-Sam1 and EphA2-Sam are providing the ML and EH binding interfaces respectively. Intermolecular interactions mainly include a

network of H-bonds and electrostatic contacts between positively charged residues of EphA2-Sam and negatively charged residues of Odin-Sam1 (Figure 5A, and Supplemental Figure S3). Cation-π and π-π interactions also occur in a few Haddock solutions and involve mainly Phe58 on the surface of Odin-Sam1 and to a lesser extent Tyr81 (EphA2-Sam EH site) and Phe53 (Odin-Sam1 ML site) (Figure 5A, and Supplemental Figure S3).

DISCUSSION

EphA2 receptor tyrosine kinase is considered a promising target in drug discovery for cancer therapies and the process of receptor endocytosis has been exploited as a possible route to reduce tumor malignancy (1). Recent evidence has shown that Sam domains are crucial for anchorage of protein regulators of endocytosis at the receptor site (8–9).

The Sam domain of lipid phosphatase Ship2 is engaged in a heterotypic interaction with the Sam domain of the receptor and is able to inhibit its endocytosis in cancer cells (8). Proteins of the ANKS family also play a prominent role in the process through their Sam domains, possibly by regulating ubiquitination mechanisms (9).

In this study we focus our attention on Odin (16), an ANKS family member that in cancer cells increases receptor stability (39).

Odin contains at the C-terminal side two Sam domains in tandem, Odin-Sam1 and Odin-Sam2. We attempted to express both isolated Sam domains (data not shown), but we could obtain only soluble Odin-Sam1 protein. However, difficulties were previously encountered for expression of the Sam2 domain of AIDA1b, another member of the ANKS protein family with high sequence homology with Odin (9, 34). For Odin-Sam1 we conducted a complete structural characterization by NMR.

Sam domains exhibit generally weak tendency to associate in solution through homotypic interactions (12, 18, 40). Our studies on the aggregation state of Odin-Sam1 confirm this trend. In fact, the correlation time of Odin-Sam1 (τc= 7.3 ns at a protein concentration of 900 μM), evaluated by ^{15}N relaxation data, is rather close to that reported for monomeric Sam domains such as Ship2-Sam (6.7 ns) (12) and Arap3(Arf GAP, Rho GAP, Ankyrin repeat and PH domain)-Sam (8.2 ns) at similar concentrations and under similar buffer conditions (18). The presence of one single Odin-Sam1 monomeric specie in solution is further supported by DOSY experiments (23). In particular, the hydrodynamic radius of the protein (i.e: ~17 Å) measured by DOSY (23), is comparable with that of compact proteins of similar size (41).

The correlation time of Odin-Sam1 bound to EphA2-Sam increases instead to ~11 ns, thus reflecting the increase in molecular weight upon association, and suggesting that the two proteins may bind with a 1:1 stoichiometry (12, 18, 34), in fact, for the AIDA1-Sam1/Sam2 tandem a similar correlation time value equal to 9.1 ns has been reported (34).

To identify closely related Sam domains, we conducted a *blastp* search against the PDB database (42) by using Odin-Sam1 sequence as input query (Supplemental Figure S4). The results show that Odin-Sam1 presents highest sequence identity (57%) with AIDA1-Sam1 (pdb id: 2EAM, Riken Structural Genomic Initiative) however, it possesses good homology also with Ship2-Sam (48% sequence identity, pdb id: 2K4P (12)) and EphA2-Sam (31% sequence identity, pdb id: 2E8N). A similar *blastp* search of Odin-Sam2 sequence indicates the highest identity with AIDA1-Sam2 (59%); sequence identities with EphA2-Sam and Ship2-Sam are instead 38% and 20% respectively (Supplemental Figure S4). In agreement with the high levels of homology revealed by *blastp*, Odin-Sam1 (Figure 1) presents the canonical Sam domain fold and its structure is rather similar to that of AIDA1-Sam1 (pdb

ids: 2EAM, 2KE7), in fact differences can be revealed only in the intrinsically disordered regions.

The Interaction between Odin-Sam1 and EphA2-Sam and comparison with other heterotypic Sam-Sam associations

Because of the high sequence identity between Ship2-Sam and Odin-Sam1 as well as the common function of regulators of EphA2 endocytosis, we have investigated if Odin-Sam1 could directly bind EphA2-Sam as Ship2-Sam does.

The interaction between Odin-Sam1 and EphA2-Sam has been studied by SPR, ITC and NMR experiments. A clear association of the two proteins is evident from analysis of all the different binding assays. The dissociation constant estimated by SPR is in good agreement with that obtained by ITC (Figure 4). ITC data also clearly indicate, in agreement with the relaxation data, that the two Sam domains bind according to a single binding site model (Figure 4C).

NMR chemical shift perturbation experiments (Figures 2 and 3) have revealed the reciprocal binding surfaces of the proteins and suggested that they may adopt a Mid-Loop (ML)/End-Helix (EH) binding mode (43). By having available the 3D structures of both Odin-Sam1 (pdb id: 2LMR) and EphA2-Sam (pdb id: 2E8N) and to recognize possible key intermolecular interactions stabilizing the complex, we have conducted molecular docking studies with the Haddock webserver (32). Docking trials have been coupled to mutagenesis studies. The latter indicate that Tyr81, Lys38 and Arg78 on the EH surface of EphA2 are likely providing important interactions, in fact, concurrent mutations of Tyr to Ser, Lys and Arg to Ala, attenuate the binding affinity for Odin-Sam1 (Supplemental Figure S1). Indeed, in most of our docking solutions these residues are involved in intermolecular contacts (Figure 5 and Supplemental Figure S3). The K38A, R78A, Y81S mutations in EphA2-Sam also decrease the binding affinity of the receptor for Ship2-Sam (12). We have previously reported on the NMR solution structure of Ship2-Sam and characterized its binding to EphA2-Sam with NMR and ITC techniques (12). These earlier studies have pointed out that Ship2-Sam and EphA2-Sam bind to each other by adopting a ML/EH binding topology (12); very recently the same interaction has been studied under different experimental conditions and the structural details of the binding interface have been further elucidated (44).

The Ship2-Sam/EphA2-Sam binding mode and the type of possible stabilizing interactions (12, 44) appear similar to that we can observe for the Odin-Sam1/EphA2-Sam complex. Indeed, an NMR based-displacement experiment shows that Ship2-Sam and Odin-Sam1 share a common binding site on the surface of the receptor (Supplemental Figure S5).

Next, we have compared our Odin-Sam1/EphA2-Sam model with the NMR structure of the tandem Sam domain of AIDA1 (pdb id: 2KIV, (34)) (Figure 5B). Analogies between the two Sam-Sam associations are evident. Interestingly, the tandem presents a Mid-Loop/End-Helix topology in which AIDA1-Sam1 and AIDA1-Sam2 are supplying the ML and EH binding surfaces respectively (34) (Figure 5A).

On the basis of the high degree of sequence homology between AIDA1 and Odin (See above), we suppose that the two Odin Sam domains in tandem may bind with an analogue ML/EH topology in which Odin-Sam1 supplies the ML interface. It is clear that if the ML surface of Odin-Sam1 is engaged in the interaction with Odin-Sam2 in the full length protein, uncoupling of the Sam2 domain from the tandem may be needed to permit binding of Sam1 to EphA2-Sam. Indeed, it has already been hypothesized that the opening of AIDA1-tandem is required for translocation of AIDA-1 toward the nucleus (34).

However, more structural and biochemical studies are needed to shed light on the complex mechanisms regulating the network of interactions of Odin and EphA2-Sam.

Moreover, it's worth noting that recent findings have associated a few mutations in EphA2-Sam with cataracts (6, 45). Some of these EphA2-Sam mutations are located close to the EH interface (i.d: the α4α5 loop and the C-terminal portion of helix α5) (Supplemental Figure S4B) whether they may cause perturbation in the structure of the receptor Sam domain and thus influence its binding affinity for Odin-Sam1 remains to be addressed.

In this regard, it could be appealing to design, based on the structural information we have obtained here and in our previous work, novel molecular probes (small molecules or peptides) able to antagonize Odin-Sam1/EphA2-Sam association and study the outcomes in a cellular context thus fully validating its relevance to either cancer or cataracts.

Supplementary Material

Refer to Web version on PubMed Central for supplementary material.

Acknowledgments

Financial support was obtained thanks to NIH grant CA138390 to M. Pellecchia and FIRB contract RBAP114AMK.

The authors thank Mr L. Zona, Mr L. De Luca and Dr. G. Perretta for technical assistance.

Abbreviations

Arap3	Arf GAP, Rho GAP, Ankyrin repeat and PH domain
AIDA1b	AβPP intracellular domain-associated protein 1B
AIDA1-Sam1	first Sam domain of AIDA1b
AIDA1-Sam2	second Sam domain of AIDA1b
ANKS	Ankyrin repeat and sterile alpha motif domain protein
DOSY	Diffusion Ordered Spectroscopy
EH	End-Helix
EphA2	Ephrin A2 receptor
EphA2-Sam	Sam domain of the EphA2 receptor
ITC	Isothermal Titration Calorimetry
HSQC	Heteronuclear Single Quantum Coherence Spectroscopy
MD	Mid-Loop
NOESY	Nuclear Overhauser Enhancement Spectroscopy
Odin-Sam1	first Sam domain of Odin
Odin-Sam2	second Sam domain of Odin
PTB Domain	Phosphotyrosine Binding Domain
Ship2	Src homology 2 domain-containing phosphoinositide-5-phosphatase 2
Ship2-Sam	Sam domain of Ship2
SPR	Surface Plasmon Resonance

TOCSY Total Correlation Spectroscopy

References

1. Pasquale EB. Eph receptors and ephrins in cancer: bidirectional signalling and beyond. Nat Rev Cancer. 2010; 10:165–180. [PubMed: 20179713]
2. Surawska H, Ma PC, Salgia R. The role of ephrins and Eph receptors in cancer. Cytokine Growth Factor Rev. 2004; 15:419–433. [PubMed: 15561600]
3. Koolpe M, Dail M, Pasquale EB. An ephrin mimetic peptide that selectively targets the EphA2 receptor. J Biol Chem. 2002; 277:46974–46979. [PubMed: 12351647]
4. Cooper MA, Son AI, Komlos D, Sun Y, Kleiman NJ, Zhou R. Loss of ephrin-A5 function disrupts lens fiber cell packing and leads to cataract. Proc Natl Acad Sci U S A. 2008; 105:16620–16625. [PubMed: 18948590]
5. Jun G, Guo H, Klein BE, Klein R, Wang JJ, Mitchell P, Miao H, Lee KE, Joshi T, Buck M, Chugha P, Bardenstein D, Klein AP, Bailey-Wilson JE, Gong X, Spector TD, Andrew T, Hammond CJ, Elston RC, Iyengar SK, Wang B. EPHA2 is associated with age-related cortical cataract in mice and humans. PLoS Genet. 2009; 5:e1000584. [PubMed: 19649315]
6. Zhang T, Hua R, Xiao W, Burdon KP, Bhattacharya SS, Craig JE, Shang D, Zhao X, Mackey DA, Moore AT, Luo Y, Zhang J, Zhang X. Mutations of the EPHA2 receptor tyrosine kinase gene cause autosomal dominant congenital cataract. Hum Mutat. 2009; 30:E603–611. [PubMed: 19306328]
7. Lupberger J, Zeisel MB, Xiao F, Thumann C, Fofana I, Zona L, Davis C, Mee CJ, Turek M, Gorke S, Royer C, Fischer B, Zahid MN, Lavillette D, Fresquet J, Cosset FL, Rothenberg SM, Pietschmann T, Patel AH, Pessaux P, Doffoel M, Raffelsberger W, Poch O, McKeating JA, Brino L, Baumert TF. EGFR and EphA2 are host factors for hepatitis C virus entry and possible targets for antiviral therapy. Nat Med. 2011; 17:589–595. [PubMed: 21516087]
8. Zhuang G, Hunter S, Hwang Y, Chen J. Regulation of EphA2 receptor endocytosis by SHIP2 lipid phosphatase via phosphatidylinositol 3-Kinase-dependent Rac1 activation. J Biol Chem. 2007; 282:2683–2694. [PubMed: 17135240]
9. Kim J, Lee H, Kim Y, Yoo S, Park E, Park S. The SAM domains of Anks family proteins are critically involved in modulating the degradation of EphA receptors. Mol Cell Biol. 2010; 30:1582–1592. [PubMed: 20100865]
10. Kim CA, Bowie JU. SAM domains: uniform structure, diversity of function. Trends Biochem Sci. 2003; 28:625–628. [PubMed: 14659692]
11. Meruelo AD, Bowie JU. Identifying polymer-forming SAM domains. Proteins. 2009; 74:1–5. [PubMed: 18831011]
12. Leone M, Cellitti J, Pellecchia M. NMR studies of a heterotypic Sam-Sam domain association: the interaction between the lipid phosphatase Ship2 and the EphA2 receptor. Biochemistry. 2008; 47:12721–12728. [PubMed: 18991394]
13. Rajakulendran T, Sahmi M, Kurinov I, Tyers M, Therrien M, Sicheri F. CNK and HYP form a discrete dimer by their SAM domains to mediate RAF kinase signaling. Proc Natl Acad Sci U S A. 2008; 105:2836–2841. [PubMed: 18287031]
14. Ramachander R, Bowie JU. SAM domains can utilize similar surfaces for the formation of polymers and closed oligomers. J Mol Biol. 2004; 342:1353–1358. [PubMed: 15364564]
15. Wei Z, Zheng S, Spangler SA, Yu C, Hoogenraad CC, Zhang M. Liprin-mediated large signaling complex organization revealed by the liprin-alpha/CASK and liprin-alpha/liprin-beta complex structures. Mol Cell. 2011; 43:586–598. [PubMed: 21855798]
16. Emaduddin M, Edelmann MJ, Kessler BM, Feller SM. Odin (ANKS1A) is a Src family kinase target in colorectal cancer cells. Cell Commun Signal. 2008; 6:7. [PubMed: 18844995]
17. Ghersi E, Vito P, Lopez P, Abdallah M, D'Adamio L. The intracellular localization of amyloid beta protein precursor (AbetaPP) intracellular domain associated protein-1 (AIDA-1) is regulated by AbetaPP and alternative splicing. J Alzheimers Dis. 2004; 6:67–78. [PubMed: 15004329]

18. Leone M, Cellitti J, Pellecchia M. The Sam domain of the lipid phosphatase Ship2 adopts a common model to interact with Arap3-Sam and EphA2-Sam. BMC Struct Biol. 2009; 9:59. [PubMed: 19765305]
19. Neri D, Szyperski T, Otting G, Senn H, Wuthrich K. Stereospecific nuclear magnetic resonance assignments of the methyl groups of valine and leucine in the DNA-binding domain of the 434 repressor by biosynthetically directed fractional 13C labeling. Biochemistry. 1989; 28:7510–7516. [PubMed: 2692701]
20. Grzesiek S, Bax A. Amino acid type determination in the sequential assignment procedure of uniformly 13C/15N-enriched proteins. J Biomol NMR. 1993; 3:185–204. [PubMed: 8477186]
21. Bartels C, Xia T, Billeter M, Güntert P, Wüthrich K. The program XEASY for computer-supported NMR spectral analysis of biological macromolecules. J Biomol NMR. 1995:1–10. [PubMed: 7881269]
22. Kay LE, Torchia DA, Bax A. Backbone dynamics of proteins as studied by 15N inverse detected heteronuclear NMR spectroscopy: application to staphylococcal nuclease. Biochemistry. 1989; 28:8972–8979. [PubMed: 2690953]
23. Morris K, Johnson CS. Diffusion-ordered two-dimensional nuclear magnetic resonance spectroscopy. J Am Chem Soc. 1992; 114:3139–3141.
24. Price WS. Pulsed-field gradient nuclear magnetic resonance as a tool for studying translational diffusion: Part 1. Basic theory. Concepts Magn Reson. 1997; 9:299–336.
25. Talluri S, Wagner G. An optimized 3D NOESY-HSQC. J Magn Reson B. 1996; 112:200–205. [PubMed: 8812906]
26. Kumar A, Ernst RR, Wuthrich K. A two-dimensional nuclear Overhauser enhancement (2D NOE) experiment for the elucidation of complete proton-proton cross-relaxation networks in biological macromolecules. Biochem Biophys Res Commun. 1980; 95:1–6. [PubMed: 7417242]
27. Herrmann T, Guntert P, Wuthrich K. Protein NMR structure determination with automated NOE assignment using the new software CANDID and the torsion angle dynamics algorithm DYANA. J Mol Biol. 2002; 319:209–227. [PubMed: 12051947]
28. Koradi R, Billeter M, Wuthrich K. MOLMOL: a program for display and analysis of macromolecular structures. J Mol Graph. 1996; 14:51–55. 29–32. [PubMed: 8744573]
29. Sanner MF, Olson AJ, Spehner JC. Reduced surface: an efficient way to compute molecular surfaces. Biopolymers. 1996; 38:305–320. [PubMed: 8906967]
30. Johnsson B, Lofas S, Lindquist G. Immobilization of proteins to a carboxymethyldextran-modified gold surface for biospecific interaction analysis in surface plasmon resonance sensors. Anal Biochem. 1991; 198:268–277. [PubMed: 1724720]
31. Rich RL, Myszka DG. BIACORE J: a new platform for routine biomolecular interaction analysis. J Mol Recognit. 2001; 14:223–228. [PubMed: 11500968]
32. de Vries SJ, van Dijk M, Bonvin AM. The HADDOCK web server for data-driven biomolecular docking. Nat Protoc. 2010; 5:883–897. [PubMed: 20431534]
33. van Dijk AD, Bonvin AM. Solvated docking: introducing water into the modelling of biomolecular complexes. Bioinformatics. 2006; 22:2340–2347. [PubMed: 16899489]
34. Kurabi A, Brener S, Mobli M, Kwan JJ, Donaldson LW. A nuclear localization signal at the SAM-SAM domain interface of AIDA-1 suggests a requirement for domain uncoupling prior to nuclear import. J Mol Biol. 2009; 392:1168–1177. [PubMed: 19666031]
35. Pellecchia M. Solution nuclear magnetic resonance spectroscopy techniques for probing intermolecular interactions. Chem Biol. 2005; 12:961–971. [PubMed: 16183020]
36. Farmer BT 2nd, Constantine KL, Goldfarb V, Friedrichs MS, Wittekind M, Yanchunas J Jr, Robertson JG, Mueller L. Localizing the NADP+ binding site on the MurB enzyme by NMR. Nat Struct Biol. 1996; 3:995–997. [PubMed: 8946851]
37. Stafford RL, Hinde E, Knight MJ, Pennella MA, Ear J, Digman MA, Gratton E, Bowie JU. Tandem SAM Domain Structure of Human Caskin1: A Presynaptic, Self-Assembling Scaffold for CASK. Structure. 2011; 19:1826–1836. [PubMed: 22153505]
38. Dominguez C, Boelens R, Bonvin AM. HADDOCK: a protein-protein docking approach based on biochemical or biophysical information. J Am Chem Soc. 2003; 125:1731–1737. [PubMed: 12580598]

39. Zhuang G, Brantley-Sieders DM, Vaught D, Yu J, Xie L, Wells S, Jackson D, Muraoka-Cook R, Arteaga C, Chen J. Elevation of receptor tyrosine kinase EphA2 mediates resistance to trastuzumab therapy. Cancer Res. 2010; 70:299–308. [PubMed: 20028874]
40. Thanos CD, Faham S, Goodwill KE, Cascio D, Phillips M, Bowie JU. Monomeric structure of the human EphB2 sterile alpha motif domain. J Biol Chem. 1999; 274:37301–37306. [PubMed: 10601296]
41. Wilkins DK, Grimshaw SB, Receveur V, Dobson CM, Jones JA, Smith LJ. Hydrodynamic radii of native and denatured proteins measured by pulse field gradient NMR techniques. Biochemistry. 1999; 38:16424–16431. [PubMed: 10600103]
42. Altschul SF, Madden TL, Schaffer AA, Zhang J, Zhang Z, Miller W, Lipman DJ. Gapped BLAST and PSI-BLAST: a new generation of protein database search programs. Nucleic Acids Res. 1997; 25:3389–3402. [PubMed: 9254694]
43. Kim CA, Gingery M, Pilpa RM, Bowie JU. The SAM domain of polyhomeotic forms a helical polymer. Nat Struct Biol. 2002; 9:453–457. [PubMed: 11992127]
44. Lee HJ, Hota PK, Chugha P, Guo H, Miao H, Zhang L, Kim SJ, Stetzik L, Wang BC, Buck M. NMR Structure of a Heterodimeric SAM:SAM Complex: Characterization and Manipulation of EphA2 Binding Reveal New Cellular Functions of SHIP2. Structure. 2012; 20:41–55. [PubMed: 22244754]
45. Shiels A, Bennett TM, Knopf HL, Maraini G, Li A, Jiao X, Hejtmancik JF. The EPHA2 gene is associated with cataracts linked to chromosome 1p. Mol Vis. 2008; 14:2042–2055. [PubMed: 19005574]
46. Laskowski RA, Rullmannn JA, MacArthur MW, Kaptein R, Thornton JM. AQUA and PROCHECK-NMR: programs for checking the quality of protein structures solved by NMR. J Biomol NMR. 1996; 8:477–486. [PubMed: 9008363]

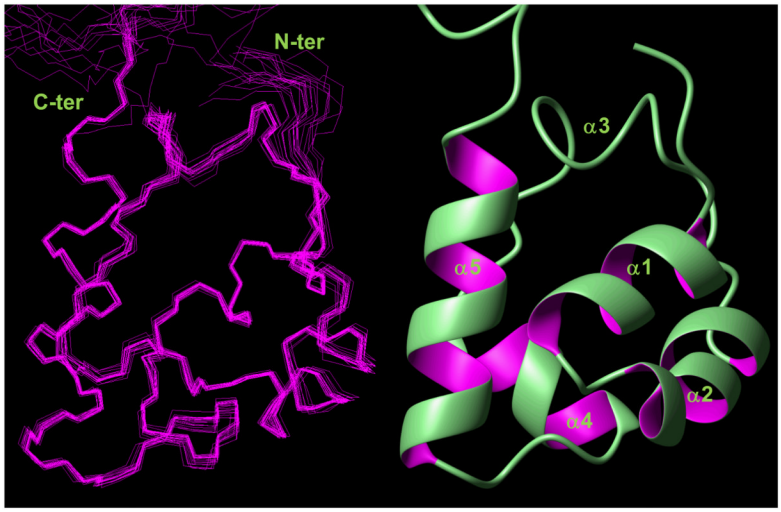

Figure 1.

Left panel. Superposition of the backbone atoms (residues 30–90) of Odin-Sam1 NMR structures. *Right panel.* Odin-Sam1, first conformer, is shown in ribbon representation including the following α helical segments: α1 (residues 32–39), α2 (residues 42–50), α4 (residues 66–72), α5 (residues 77–88). The disordered N-terminal tail encompassing residues 21–27 has been omitted from the Figure for the sake of clarity.

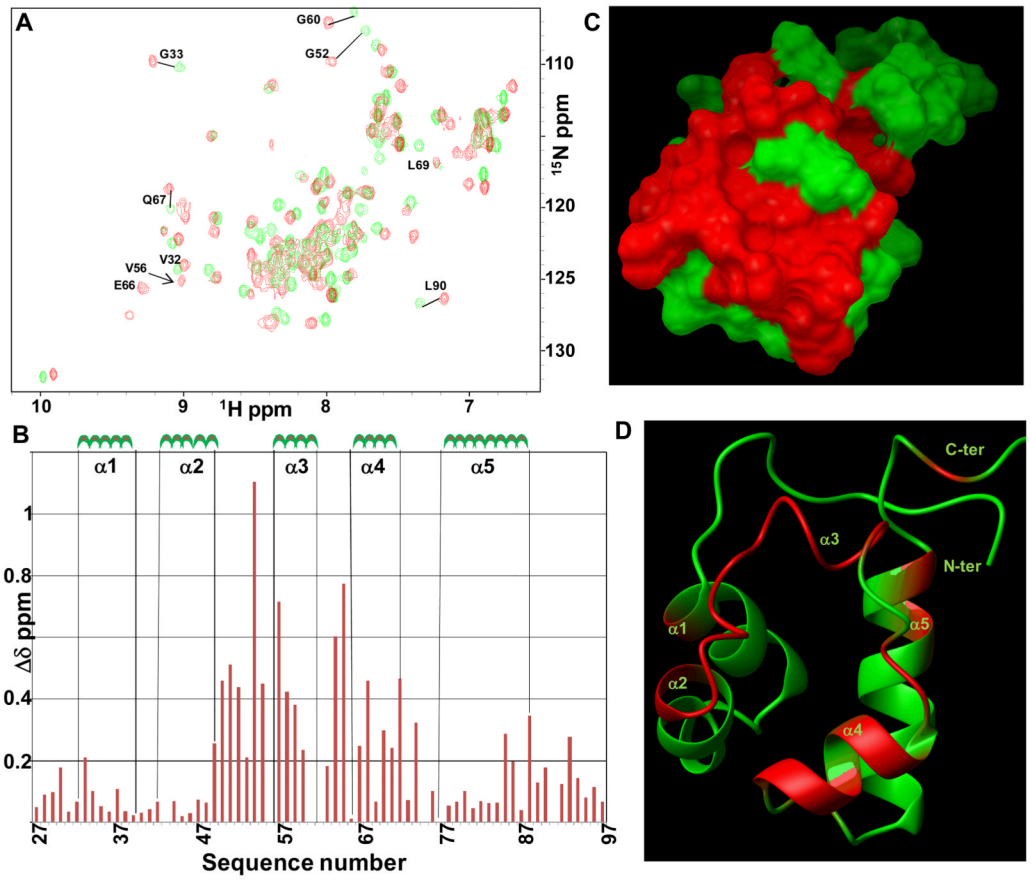

Figure 2.

A. Overlay of [^{1}H, ^{15}N] HSQC spectra of Odin-Sam1 (150 μM) before (green) and after addition of EphA2-Sam (363μM) (red). *B.* Graph of chemical shift deviations ($\Delta\delta=[(\Delta H_N)^2 + (0.17 *\Delta^{15}N)^2]^{1/2}$) *versus* residue number. A Δδ value equal to 0 has been assigned to residues Q43, V56, N62, whose peaks can be only seen in the spectrum of Odin-Sam1 bound to EphA2-Sam, S61 and S75 (unassigned), P77 and P91. *C, D.* Surface (*C*) and ribbon (*D*) representations of Odin-Sam1 (conformer number 1); residues with Δδ values higher than 0.2 ppm (i.e G33, L49, L50, N51, G52, F53, D54, D55, H57, F58, L59, G60, M64, E65, Q67, D68, R70, D71, I72, I74, Q85, R88, V93) are colored red.

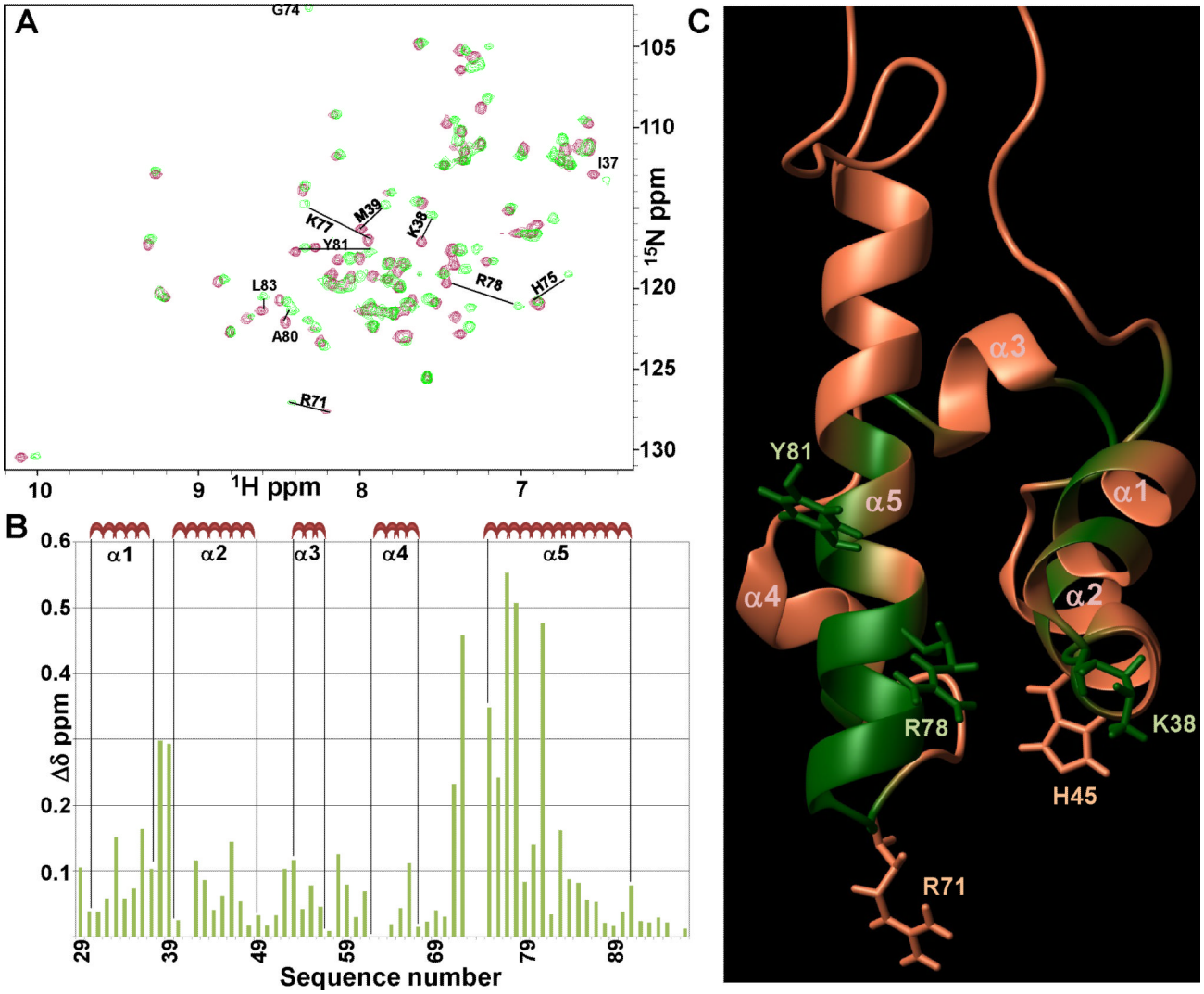

Figure 3.

A. Superposition of [^{1}H, ^{15}N] HSQC spectra of EphA2-Sam (63 μM concentration) in the apo form (maroon) and bound to Odin-Sam1 (330 μM) (green). *B.* Histogram of normalized chemical shift deviations *versus* residue number. The largest variations (Δδ values > 0.1 ppm) are observed for residues T29, W33, S36, I37, K38, M39, Y42, F46, T52, A53, V58, K66, R71, L72, H75, Q76, K77, R78, A80, Y81, L83. Data are set equal to 0 for residues N62 and D63 (unassigned), G74, Q41 (their peaks are visible only in the spectrum of the bound protein), P73 and P96. *C.* Ribbon representation of EphA2-Sam (conformer number 1, pdb id: 2E8N, from RIKEN Structural Genomics Initiative); residues presenting Δδ values > 0.1 ppm are colored green. Side chains of amino acids involved in mutagenesis studies are colored green (EphA2-Sam triple mutant) and coral (EphA2-Sam double mutant).

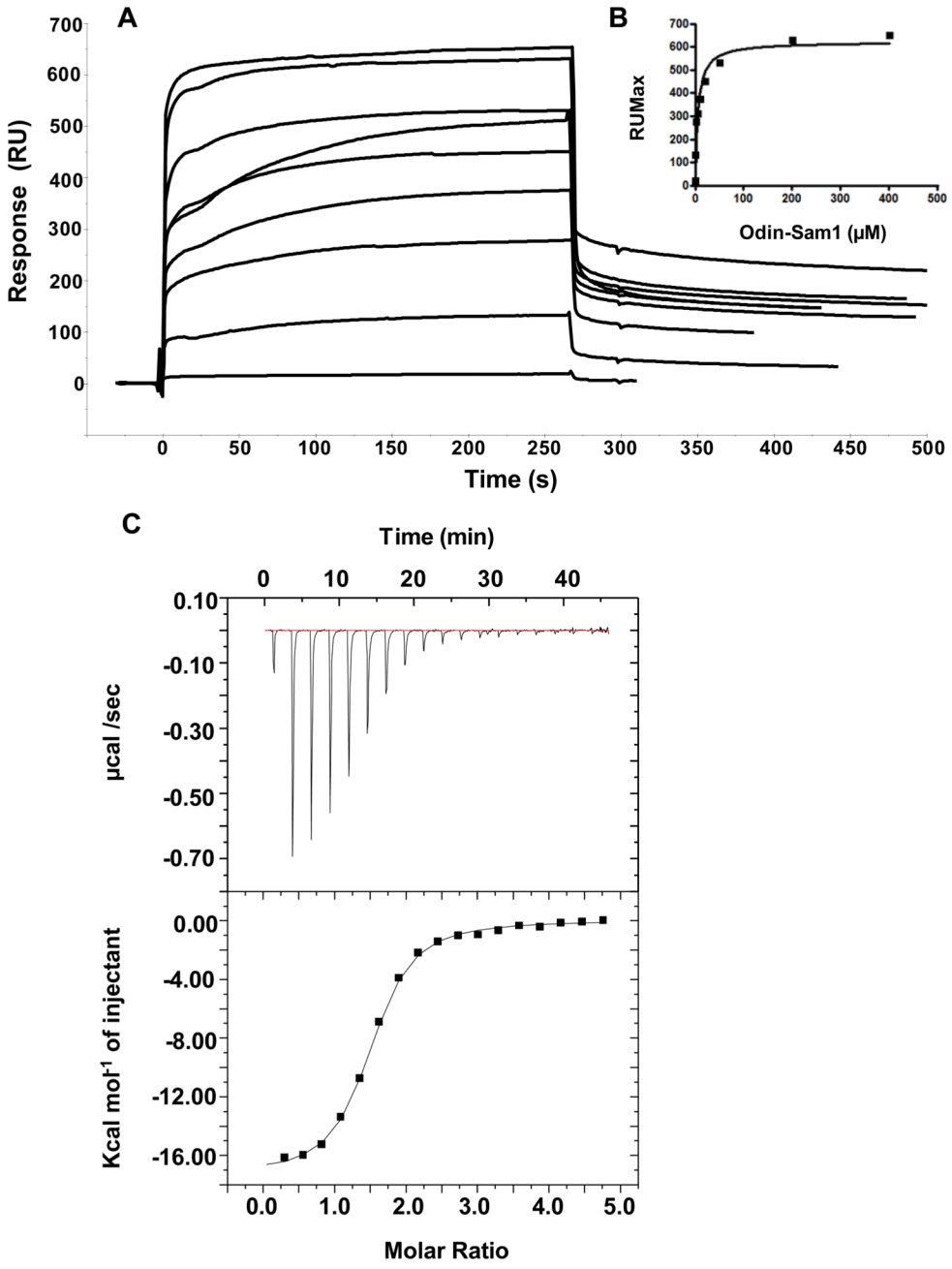

Figure 4.

A, B SPR Studies. Overlay of sensorgrams relative to the direct binding of Odin-Sam1 to immobilized EphA2-Sam (0.1–400 μM) (*A*). Plot of RU_{max} from each binding versus Odin-Sam1 concentrations (*B*); data were fit by non-linear regression analysis. *C.* ITC Studies. Calorimetric curve showing EphA2-Sam (257 μM) titration with Odin-Sam1 (10 μM). The top and bottom sections report the raw and integrated data respectively. A single binding site model was applied for data fitting (bottom).

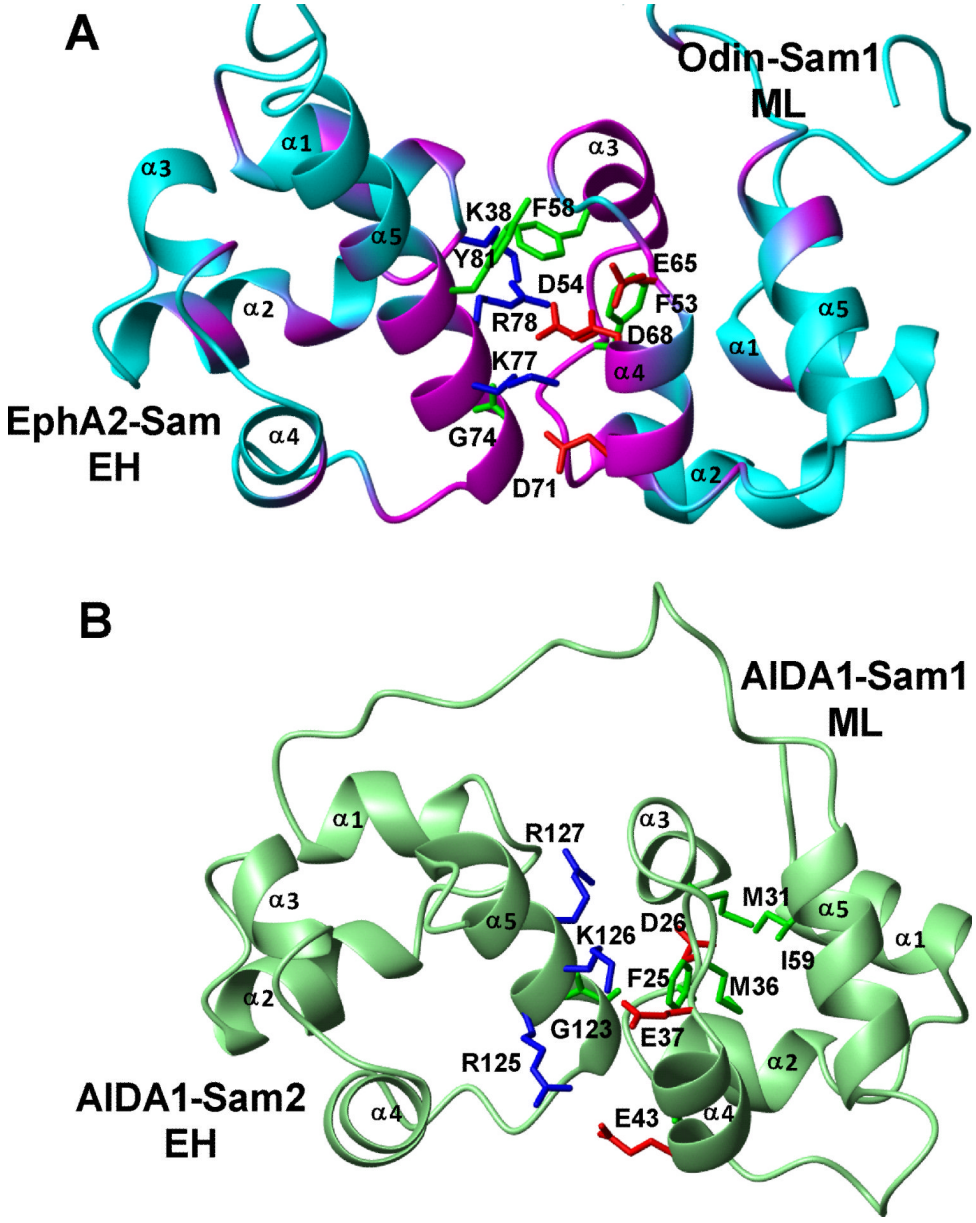

Figure 5.

A. Model of the Odin-Sam1/EphA2-Sam complex (second Haddock ranked structure belonging to the most populated docking cluster1). Protein regions with the largest chemical shift variations upon Sam-Sam association, according to NMR chemical shift perturbation experiments, are highlighted in magenta and a subset of the amino acids providing interactions at the dimer interface are indicated. *B.* NMR structure of the AIDA-1 Sam domain tandem (pdb id: 2KIV, structure n.1) (34). Most of the residues belonging to the ML and EH interfaces of Sam1 and Sam2 are shown (34).

Table 1

Statistics for Odin-Sam1 solution structure

NOE upper distance limits	1206
Angle constraints	372
Residual target function, Å^2	0.79±0.08
Residual NOE violations	
Number > 0.1 Å[#]	2
Maximum, Å	0.205±0.07
Residual angle violations	
Number	0
Atomic pairwise RMSD, Å	
Backbone atoms (aa 30–90)	0.26±0.07
Heavy atoms (aa 30–90)	0.74±0.09
Procheck analysis [@]	
Residues in core regions	84.6%
Residues in allowed regions	15.1%
Residues in generous regions	0.3%
Residues in disallowed regions	0 %

[#]Maximum CYANA (27) violations

[@]PROCHECK_NMR (46) statistics for residues 30–90